REPORT DOCUMENTATION PAGE	Form Approved OMB NO. 0704-0188

1. REPORT DATE (DD-MM-YYYY)	2. REPORT TYPE	3. DATES COVERED (From - To)
29-01-2013	Final Report	1-Oct-2009 - 31-Mar-2012

4. TITLE AND SUBTITLE
Direct Methanol Fuel Cell (DMFC) Battery Replacement Program

5a. CONTRACT NUMBER

5b. GRANT NUMBER
W911NF-09-C-0155

5c. PROGRAM ELEMENT NUMBER
622705

6. AUTHORS
Dr. Michele Tague

5d. PROJECT NUMBER

5e. TASK NUMBER

5f. WORK UNIT NUMBER

7. PERFORMING ORGANIZATION NAMES AND ADDRESSES
NuVant Systems, Inc.
9800 Connecticut Dr.

Crown Point, IN   46307 -

8. PERFORMING ORGANIZATION REPORT NUMBER

9. SPONSORING/MONITORING AGENCY NAME(S) AND ADDRESS(ES)
U.S. Army Research Office
P.O. Box 12211
Research Triangle Park, NC 27709-2211

10. SPONSOR/MONITOR'S ACRONYM(S)
ARO

11. SPONSOR/MONITOR'S REPORT NUMBER(S)
57258-CH.2

12. DISTRIBUTION AVAILIBILITY STATEMENT
Approved for Public Release; Distribution Unlimited

13. SUPPLEMENTARY NOTES
The views, opinions and/or findings contained in this report are those of the author(s) and should not contrued as an official Department of the Army position, policy or decision, unless so designated by other documentation.

14. ABSTRACT
Active DMFCs require complicated balance of plant to ensure recirculation of unreacted methanol and internally produced water as well as venting of exhaust gases. An alternative approach is redesign of the fuel delivery system to accommodate concentrated methanol that is consumed entirely within the fuel cell, thus removing the need for recirculation. A specialized anodic porous structure was designed which the dual role of flowfield and diffusion medium for concentrated methanol. In addition, a highly hydrophobic gas diffusion media were used at the DMFC

15. SUBJECT TERMS
direct methanol fuel cell, battery replacement

16. SECURITY CLASSIFICATION OF:			17. LIMITATION OF ABSTRACT	15. NUMBER OF PAGES	19a. NAME OF RESPONSIBLE PERSON
a. REPORT	b. ABSTRACT	c. THIS PAGE	UU		Bogdan Gurau
UU	UU	UU			19b. TELEPHONE NUMBER
					219-644-3231

Direct Methanol Fuel Cell (DMFC) Battery Replacement Program

ABSTRACT

Active DMFCs require complicated balance of plant to ensure recirculation of unreacted methanol and internally produced water as well as venting of exhaust gases. An alternative approach is redesign of the fuel delivery system to accommodate concentrated methanol that is consumed entirely within the fuel cell, thus removing the need for recirculation. A specialized anodic porous structure was designed which the dual role of flowfield and diffusion medium for concentrated methanol. In addition, a highly hydrophobic gas diffusion media were used at the DMFC cathode to prevent water loss by promoting water back-diffusion to the anode. This internally dilutes the methanol and enables use of highly concentrated methanol. The anodic porous structure used in concert with the hydrophobic cathode diffusion medium led to gross fuel energy densities of the operating cell of ca. 845 W*hr/Lfuel and fuel utilization in excess of 70%. A small 2 cell stack was built and successfully operated to verify that the concept is scalable. The hydrophobicity of the cathode diffusion layer is of vital importance for this concept and research for improved materials that will reduce water loss even more is still ongoing using internal funds. The project also funded student research at Northeastern University and at Inter American University in Puerto Rico. This hardware based program complemented an IFDL modeling program sponsored by the DOE.

Enter List of papers submitted or published that acknowledge ARO support from the start of the project to the date of this printing. List the papers, including journal references, in the following categories:

(a) Papers published in peer-reviewed journals (N/A for none)

<u>Received</u>   <u>Paper</u>

TOTAL:

Number of Papers published in peer-reviewed journals:

(b) Papers published in non-peer-reviewed journals (N/A for none)

<u>Received</u>   <u>Paper</u>

TOTAL:

Number of Papers published in non peer-reviewed journals:

(c) Presentations

Number of Presentations: 0.00

<u>Received</u>   <u>Paper</u>

TOTAL:

Number of Non Peer-Reviewed Conference Proceeding publications (other than abstracts):

Peer-Reviewed Conference Proceeding publications (other than abstracts):

<u>Received</u>   <u>Paper</u>

TOTAL:

Number of Peer-Reviewed Conference Proceeding publications (other than abstracts):

(d) Manuscripts

<u>Received</u>   <u>Paper</u>

01/24/2013   1.00   Dunesh Kumari, Corey Grice, Eugene S. Smotkin. Durability studies on performance degradation of
                     Catalysts and Nafion™ Membrane Functional Groups in Direct Methanol Fuel Cells,
                     IN PREP (06 2013)

TOTAL: **1**

Number of Manuscripts:

Books

Received	Paper

TOTAL:

Patents Submitted

Patents Awarded

Awards

Graduate Students

NAME	PERCENT_SUPPORTED	Discipline
Michael Bates	1.00	
Ian Kendrick	1.00	
Dunesh Kumari	1.00	
Adam Yakaboski	1.00	
FTE Equivalent:	**4.00**	
Total Number:	**4**	

Names of Post Doctorates

NAME	PERCENT_SUPPORTED
Michele Tague	1.00
FTE Equivalent:	**1.00**
Total Number:	**1**

Names of Faculty Supported

NAME	PERCENT_SUPPORTED
FTE Equivalent:	
Total Number:	

Names of Under Graduate students supported

NAME	PERCENT_SUPPORTED	Discipline
Mike Fuccillo	1.00	Chemistry
Matthew Webber	1.00	Physics
Jonathan Scarfo	1.00	Mechanical Engineering
Ian Alexander	1.00	Mechanical Engineering
Sara Evarts	1.00	Chemistry
FTE Equivalent:	**5.00**	
Total Number:	**5**	

Student Metrics

This section only applies to graduating undergraduates supported by this agreement in this reporting period

The number of undergraduates funded by this agreement who graduated during this period: 2.00

The number of undergraduates funded by this agreement who graduated during this period with a degree in science, mathematics, engineering, or technology fields:...... 2.00

The number of undergraduates funded by your agreement who graduated during this period and will continue to pursue a graduate or Ph.D. degree in science, mathematics, engineering, or technology fields:...... 1.00

Number of graduating undergraduates who achieved a 3.5 GPA to 4.0 (4.0 max scale):...... 2.00

Number of graduating undergraduates funded by a DoD funded Center of Excellence grant for Education, Research and Engineering:...... 0.00

The number of undergraduates funded by your agreement who graduated during this period and intend to work for the Department of Defense 0.00

The number of undergraduates funded by your agreement who graduated during this period and will receive scholarships or fellowships for further studies in science, mathematics, engineering or technology fields:...... 0.00

Names of Personnel receiving masters degrees

NAME

Emily Lewis

Joe Bedard

Total Number: **2**

Names of personnel receiving PHDs

NAME

Total Number:

Names of other research staff

NAME   PERCENT_SUPPORTED

FTE Equivalent:

Total Number:

Sub Contractors (DD882)

Inventions (DD882)

Scientific Progress

Technology Transfer

AWARD NUMBER

W911NF-09-C-0155

SUBMITTED BY

NuVant Systems, Inc.

130 N. West Street

Crown Point, IN 46307

PROJECT TITLE

Direct Methanol Fuel Cell (DMFC) Battery Replacement Program

PRINCIPAL INVESTIGATOR

Bogdan Gurau,
219-644-3231
m.tague@nuvant.com

SUBMITTED TO

Army Research Office

Final Report for Project 20968 – Passive DMFC

Table of Contents

3

Table of Figures

4

Introduction

During December 2009 and March 2011 GTI acted as subcontractor to NuVant Systems, Inc. in order to aid NuVant in its efforts to develop a DMFC stack operating at elevated methanol concentrations.

NuVant's idea was to use porous plates to restrict the transport of MeOH in order to control the delivery of fuel to the DMFC anode. GTI was asked to produce the porous plates and eventually design a short, "proof-of-concept" grade stack around NuVant's idea.

The work plan for GTI, as issued by NuVant , is illustrated in the following Gantt chart.

Year	2009	2010												2011		
Month	Dec	Jan	Feb	Mar	Apr	May	Jun	Jul	Aug	Sep	Oct	Nov	Dec	Jan	Feb	Mar
TASK 1. CHARACTERIZE PORVAIR PLATE																
Subtask 1.1. Determine average pore diameter																
Subtask 1.2. Determine total porosity																
Subtask 1.3. Determine open porosity																
Subtask 1.5. Determine electrical conductivity																
Subtask 1.5. Determine hydraulic permeability																
TASK 2. PRODUCE & CHARACTERIZE POROUS PLATES WITH VARIOUS POROUS STRUCTURES																
Subtask 2.1. Produce plates with Porvair characteristics (see Task 1)																
Subtask 2.2. Produce plates with ca. 2 micron pores & ca. 25, 50 & 75% total porosity																
Subtask 2.3. Produce plates with ca. 20 micron pores & ca. 25, 50 & 75% total porosity																
Subtask 2.4. Produce plates with ca. 50 micron pores & ca. 25, 50 & 75% total porosity																
Subtask 2.5. Re-Produce plates with best performance based on results from Subtasks 2.1. - 2.4.																
Subtask 2.6. Apply various hydrophobic/hydrophilic treatments																
Subtask 2.7. Reproduce plates with hydrophobic/hydrophilic treatments																
TASK 3. PRODUCE BIPOLAR PLATES FOR A SHORT STACK																

★ Milestone evaluation followed by a "go no-go" decision

Figure 1: Gantt chart illustrating GTI's work plan and milestone evaluation

GTI's performance was evaluated at regular intervals of time and "go no-go" decisions were issued. The milestones for GTI are indicated in figure 1 by the green star and a broader description is presented below:

> **1st period** will last between beginning of project (Dec. 1st, 2009) and end of subtask 2.1. (March 15th, 2010).

Milestone#1 – Measure the characteristics and show the ability to produce porous plates with characteristics close to a commercially available porous plate

At the end of subtask 2.1., NuVant will evaluate GTI's ability to produce a porous structure with characteristics close to the Porvair material submitted to GTI as starting point. A go or no-go decision will be issued.

2nd period will last between the end of subtask 2.1. (March 15th, 2010) and the end of subtask 2.5. (July 31st, 2010).

Milestone#2 – Show the ability to produce other types of porous structures

At the end of subtask 2.5., NuVant will evaluate GTI's ability to produce porous structures with various degrees of porosity and average pore diameter. A go or no-go decision will be issued.

3rd period will last between the end of subtask 2.5. (July 31st, 2010) and the end of subtask 2.7. (Nov. 30th, 2010).

Milestone#3 – Reproduce the best performing plates and add various treatments that could potentially improve DMFC performance

By the end of Nov. 2010 NuVant should be in the position where the single cell DMFCs will be working in a satisfactory manner in terms of achieving good electrical performance (Watts) and good fuel energy density (Watt*hr/L$_{fuel}$). If that is not accomplished there is no point in attempting to build a stack (Task 3) and a "no-go" decision will be issued.

4th period will cover the remaining time of the project, namely between Nov. 30th, 2010 and March 31st, 2011.

Milestone#4 – Build a short, "proof-of-concept" grade stack

No "go no-go" decision will be issued, as the project will end.

GTI's performance in achieving the milestones described above is described in detail in the following paragraphs.

Milestones

1 – Measure the characteristics and show the ability to produce porous plates with characteristics similar to a commercially available plates.

NuVant has supplied GTI with samples of a commercially available porous plate in order to estimate GTI's ability to measure the meaningful characteristics of a porous structure. The plate supplied by NuVant was from Porvair. Tables 1-3 are properties of the Porvair plate.

Table 1: Physical properties of the Porvair plate

Plate	Average pore diameter (μm)	Median pore diameter (μm)	Bulk density (g/mL)	Skeletal density (g/mL)	Porosity (%)
Porvair	0.0424	2.76	1.26	1.84	32.5

Table 2: Electrical properties of the Porvair plate

Plate	Surface contact resistance (Gold reference) (mΩ)	Surface contact resistance (mΩ)	Bulk resistivity (Ω·cm)
Porvair	110	243	Not measured *

* Sample too small to measure

Table 3: Permeation properties of the Porvair plate

| Plate	Permeability* (kg/m·s·Pa)		
	water	6M methanol/water	methanol
Porvair disk 2	2.88 x 10-13	4.33 x 10-10	1.36 x 10-9

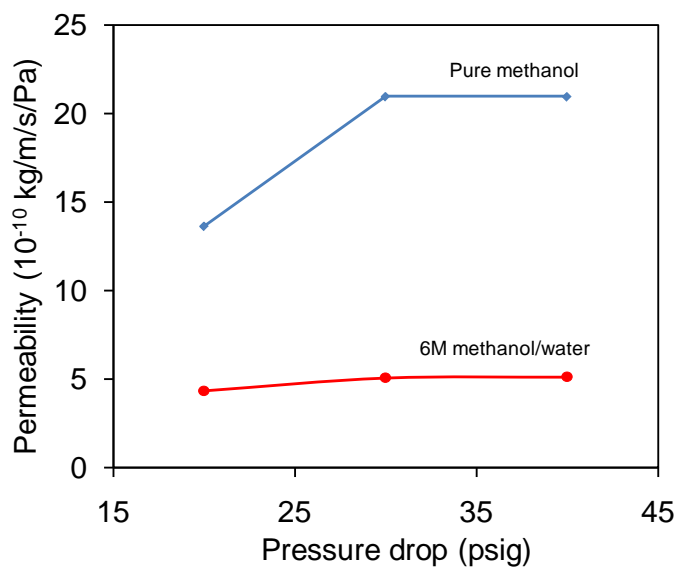* Testing conditions:
Plate thickness: 1.93 mm, Permeable area: 5.07 cm2, ΔP = 20 psig
Permeance= mass permeated/permeable area/time/pressure drop, kg/m2·s·Pa
Permeability= permeance × plate thickness, kg/m·s·Pa.

Figure 2 shows water permeability and Figure 3 shows methanol permeability as a function of pressure drop for the Porvair plate.
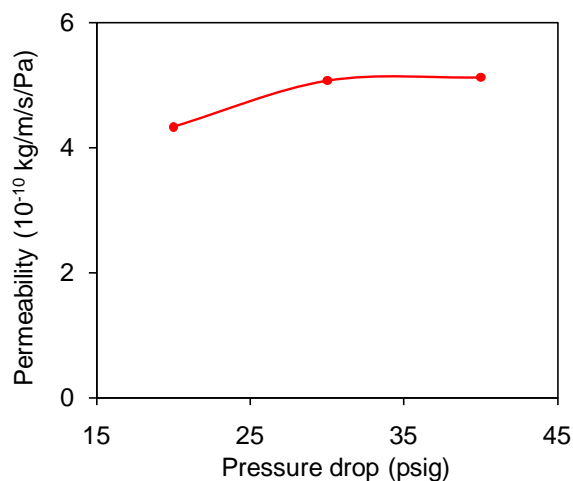
Figure 2: Water permeability

 Figure 3: Methanol permeability

NuVant was satisfied with GTI characterization of porous structures. GTI initiated production their own porous structures with characteristics improved relative to Porvair plates. The result of this work is presented in the following:

Physical properties of the GTI plates were determined by GTI Analytic Lab. Results are summarized in Table 4. The physical properties for Porvair plate are also listed in Table

4 for comparison. Detailed information for each sample is also available upon requirement. As shown in Table 4, GTI-5%-10K plate has higher porosity than Porvair plate.

Table 4: Comparison of physical properties

Plate	Average pore diameter (μm)	Median pore diameter (μm)	Bulk density (g/mL)	Skeletal density (g/mL)	Porosity (%)
Porvair	0.0424	2.76	1.26	1.84	32.5
GTI-5%-10K*	0.646	2.73	1.36	2.11	36.3
GTI-10%-10K	0.505	2.50	1.57	2.10	26.2
GTI-15%-10K	0.279	2.82	1.55	2.03	24.6

*GTI-5%-10K means GTI's plate prepared with 5% resin (binder) and pressed at 10K lbs

The milestone#1 is successfully accomplished.

#2 – Show the ability to produce other types of porous structures

Upon successful conclusion of milestone#1 NuVant expressed the desire to have porous plates of various properties with respect to pore diameter and porosity. These two parameters ultimately reflect the permeability of the plate. GTI produced and supplied NuVant with various porous plates for which it also performed the permeability measurements. The results are presented in the following:

Electrical Properties

Electrical properties of the GTI plates are summarized in Table 5. Results for the Porvair plate are also listed in Table 5 for comparison. As shown, all GTI plates had lower surface contact resistance than the Porvair plate.

Table 5: Comparison of electric properties

Plate	Surface contact resistance* (mΩ)	Volume resistivity (Ω·cm)
Porvair	243.3	-**
GTI-5%-10K	213.7	3.96×10^{-4}
GTI-10%-10K	207.9	2.86×10^{-4}
GTI-15%-10K	195.6	2.22×10^{-4}
GTI-5%-33K	206.7	1.98×10^{-4}
GTI-5%-66K	198.7	1.13×10^{-4}
GTI-5%-99K	197.8	1.12×10^{-4}
GTI-5%-132K	178.0	1.27×10^{-4}
GTI-5%-165K	172.6	1.03×10^{-4}

* During measurement for each sample, the surface contract resistance of gold was measured as reference. The values for gold were 98-110 mΩ

** Sample too small to measure.

Hydraulic Permeabilities

Hydraulic permeabilities of pure water, pure methanol, and methanol/water mixtures for the Porvair and GTI plates were measured using a system shown in Figure 4. Permeabilities

were generally measured at pressure drops of 20, 30 and 40 pisg. Note that permeability (kg/m·s·Pa) was calculated by permeance × plate thickness, where permeance (kg/m2·s·Pa) = mass permeated/permeable area/time/pressure drop.

**Figure 4: Hydraulic permeability testing system**

Figure 5 compares permeabilities for a 50/50 (vol%) methanol/water (12.5 M) of GTI plates with Porvair plate. In the pressure drop range measured, the permeabilities of Porvair plate were in between GTI plates prepared with different fraction of binder. Methanol permeate concentrations were measured by off-line GC (CARLE Series 400) equipped with a thermal conductivity detector and HAYESEP-A column. For all plates, the measured methanol concentrations in the permeate side were identical to those in the feed.
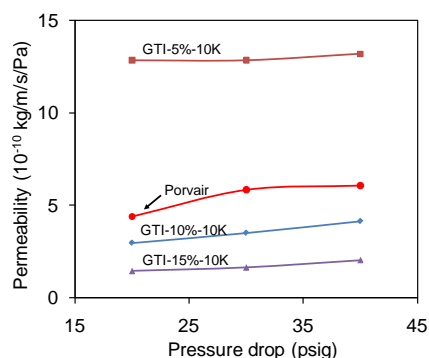
Figure 5: Permeability for 50/50 vol% methanol/water mixture

Figure 6 compares permeabilities of Porvair and GTI-5%-10K plates at a pressure drop of 20 psig for different methanol feed concentrations. Pure water, 6M, 12.5M, 17.6M methanol/water mixtures, and pure methanol feeds have been investigated. Apparently, Porvair plate was highly hydrophobic as its water permeability was much lower than the GTI-5%-10K plates.
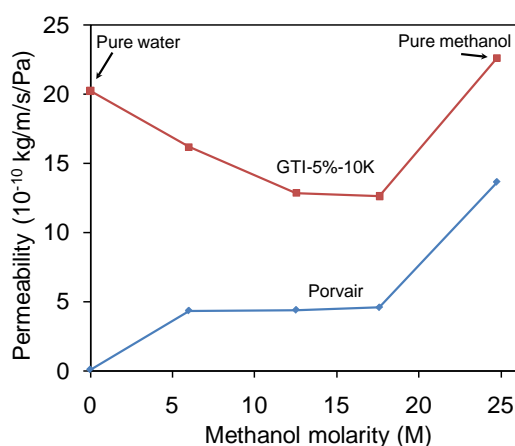
Figure 6: Permeabilities at a pressure drop of 20 psig for Porvair and GTI-5%-10K plates.

Note that the permeabilities for GTI-5%-10K plates were much higher than those for Porvair plates with all feeds measured:

• For 6M methanol/water,   PGTI-5%-10K = 3.7 times of Pporvair

• For 12.5M methanol/water (50/50 vol%),   PGTI-5%-10K = 2.9 times of Pporvair

• For 17.6M methanol/water (50/50 mol%),   PGTI-5%-10K = 2.8 times of Pporvair

• For pure methanol,   PGTI-5%-10K = 1.7 times of Pporvair

Milestone#2 was also successfully accomplished.

#3 – Reproduce the best performing plates and add various treatments that could potentially improve DMFC performance

The reproduction of the plates was not a problem and GTI supplied NuVant with repeated batches of the plates that NuVant deemed as best performing when tested in the DMFCs, all performing satisfactory.

NuVant attempted to improve the performance of certain plates by asking GTI to cover machined porous plates surfaces with a hydrophobic epoxy. Upon re-machining these plates at NuVant, the epoxy treatment would block the permeation of the methanol solutions in various areas of the plate while the re-machined areas would allow for permeation of methanol solutions.

An example of such produced plate with NuVant designed flowfield is shown in figure 7.
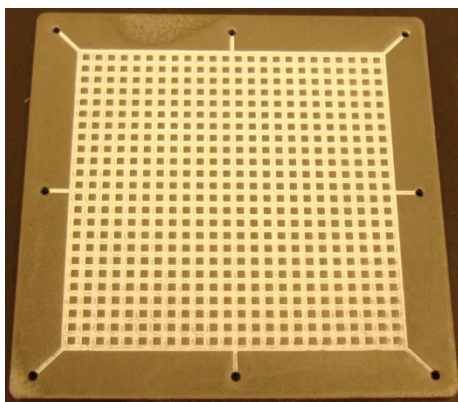

Figure 7: Epoxy blocked IFDL

For reasons that remain unknown, the epoxy treated plates showed poorer performance compared to the untreated plates and NuVant decided to abandon the treatment. However, from GTI's work statement point of view the milestone #3 has also been accomplished.


Milestone#4 – Build a short, "proof-of-concept" grade stack

GTI has built a short 2 cell stack that accommodates NuVant's technology of operation of DMFCs with elevated methanol concentrations. The constituent parts of the stack as well as the assembled stack are shown in figures 8 and 9.
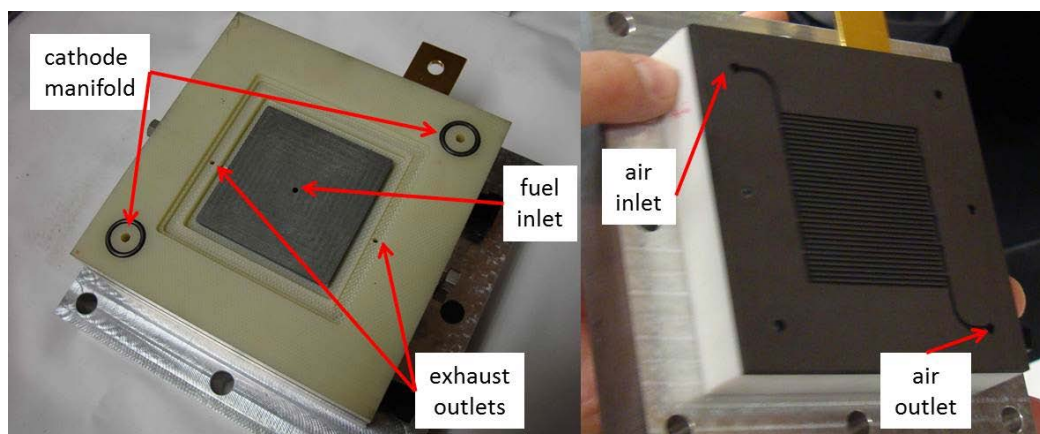
Figure 8: Exploded view of main stack constituents. Anode housing without the porous plate (left). Cathode flowfield (right)

The porous plate machined by and according to NuVant specifications is lodged inside the anode housing. The fuel enters through the middle hole, diffuses through the porous structure, reacts at the anode and the exhaust gas exits the anode housing through the 2 exhaust holes shown in the picture (left). The cathode plate is comprised of a conventional serpentine flowfield and is shown at the right in figure 8. NuVant fabricated MEAs are placed in between the two plates shown in figure 8 via additional gaskets. A view of the assembled stack is shown in figure 9.
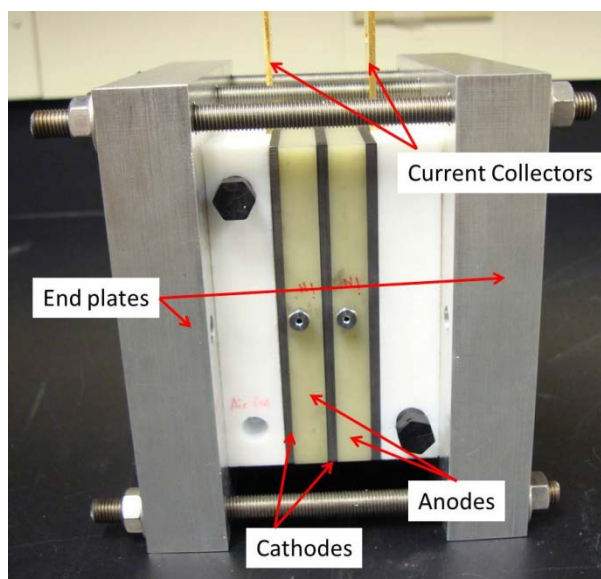
Figure 9: Assembled stack

The stack was operated with 17M MeOH solution and 400 sccm of air. A preliminary polarization curve is shown in figure 10.
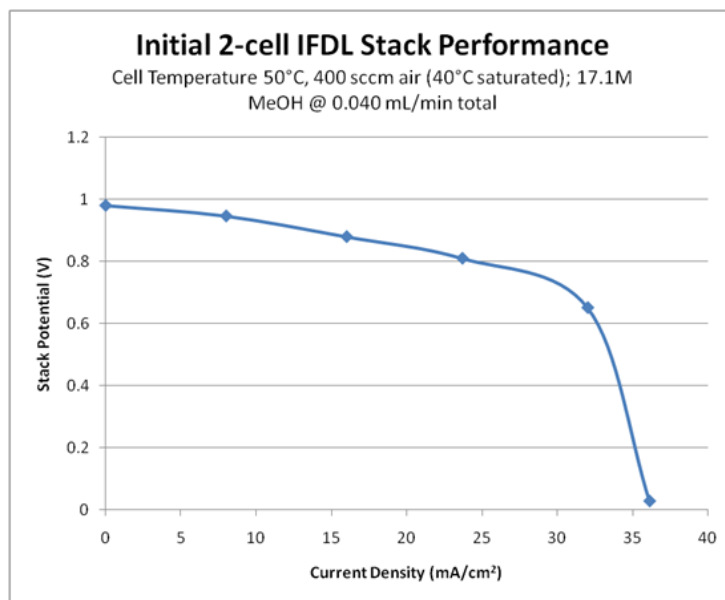
Figure 10: Preliminary performance of the short DMFC stack

Unfortunately, one of the 2 MEAs assembled inside of the DMFC stack was not performing very well and created the large mass transport drop around the 30 mA/cm² mark. The MEA will be replaced and the performance will be re-evaluated. There is no reason to expect complications as the other MEA in the stack was performing very well.

Milestone#4 and last was also successfully accomplished.

Single Cell: Internal Metrics

Legacy Mode vs. IFDL

- IFDL delivers significantly higher GFED, but only using higher MeOH conc.

- MeOH utilization comparable

- Legacy power density is slightly higher than IFDL

- Nafion 117 is not optimum membrane for IFDL configuration

Table 6: Single Cell: Internal Metrics

Operating Mode	W*h/L	MeOH Util.	mW/cm^2
Legacy (0.5M MeOH)	23.7	66.3	35.5
IFDL (0.5M MeOH)	22.1	66.3	33.2
IFDL (17.1M MeOH)	697	63.8	31.8

Nafion 117 based MEA

4mg/cm^2 Pt, PtRu black, CCM method

2.0A (80mA/cm^2), 60°C, 200 sccm air

O2:MeOH Stoich Ratio ~16

Single Cell: External Metrics

Comparison to Outside DMFC Systems

- NuVant IFDL DMFC technology appears to be comparable to many near-commercialized DMFC power systems in terms of gross fuel energy density

- Further optimization must still be accomplished for NuVant to be competitive

    - DoE target goal was 1000 Wh/L

Table 7: Single Cell: External Metrics

| Fuel Cell Project/System	GFED (W*h/L)
NuVant IFDL DMFC[1]	845
SEC JENNY[2]	800
EFOY 1600-M5[2]	577
EFOY 1600-M10[2]	650
EFOY 1600-M28[2]	607
Oorja Pac[2]	909
UltraCell XX25[2]	692
Passive DMFC Single Cell[3]	850

1. Best performance as of March 2011, 25cm[2] single cell
2. DMFC power system data; S. Narayan and T. Valdez, ECS *Interface* Winter 2008, p. 40
3. Xioaming Ren, et al. Patent # US 7541109B2, Jun 2, 2009

Single Cell: Characterization

Operating Parameter Effects

- Individual polarization curves constructed for each condition

- Peak GFED is identified from each curve

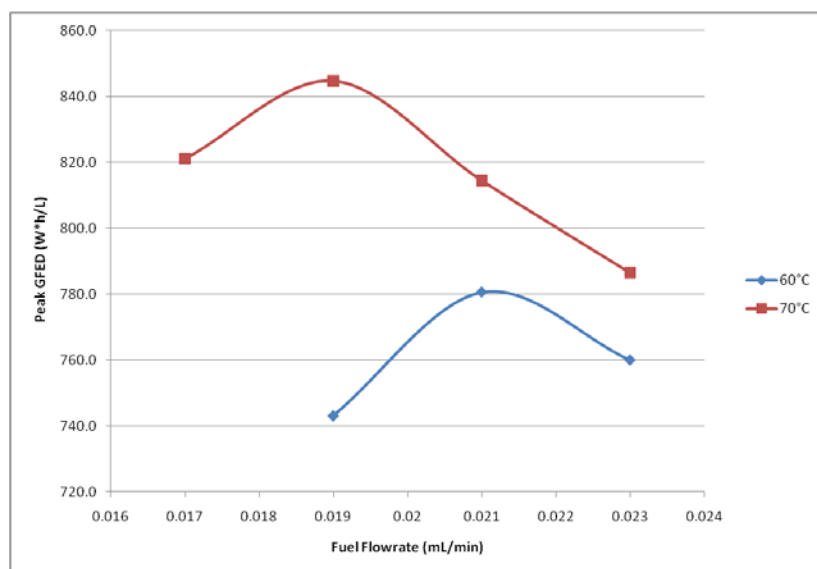**Figure 11: Single Cell: Characterization**
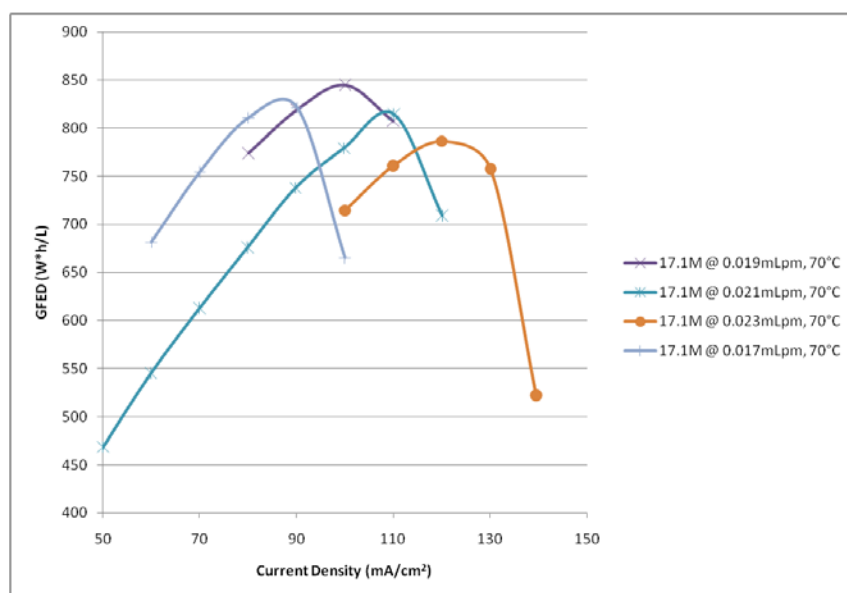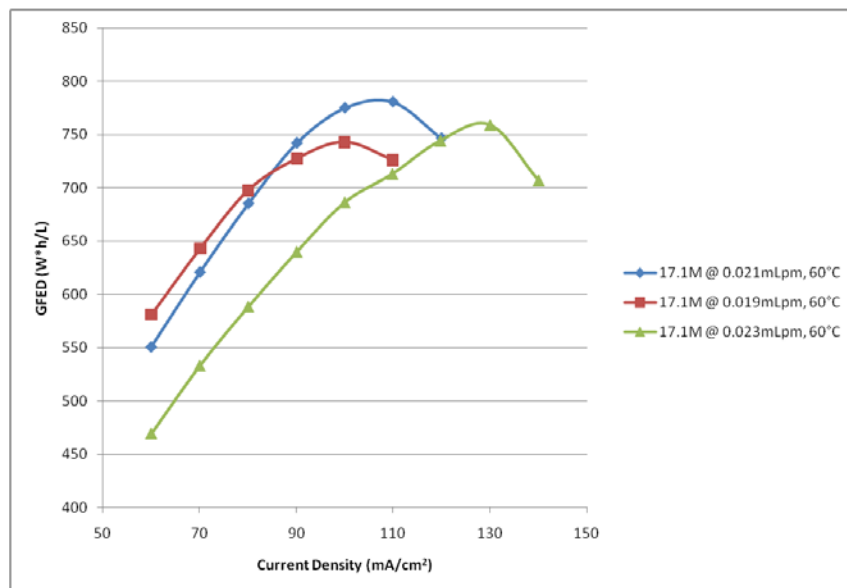
Single Cell: Optimization

Operating Parameter Effects

- Comparison of peak GFED details optimization pathway

- Characterization not complete yet

  – MeOH concentration effect not fully examined

  – Studies are still in progress
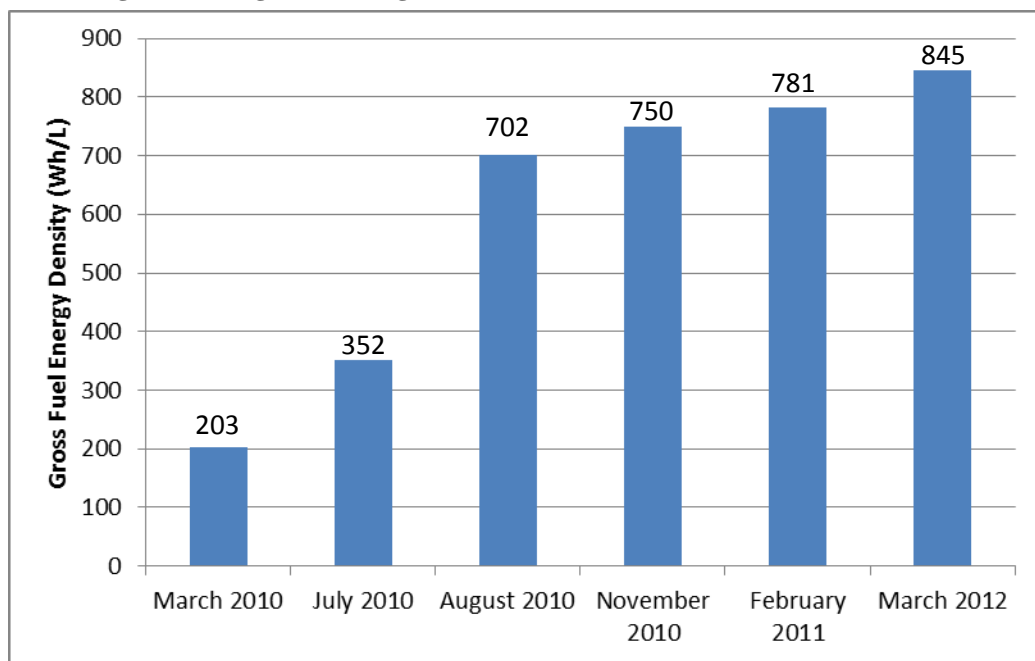
Figure 12: Single Cell: Optimization

Single Cell: Progress

GFED: Beginning Of Project Up To Present

Figure 13: Single Cell: Progress

Target: GFED of close to 1000 W*hr/L$_{fuel}$

Single Cell: Remaining Challenges

Cathode Humidification

- IFDL performance significantly improved with cathode humidification

    – Most results use 62-66% RH air

- Neither DoE/DoD project stated dry air was required

    – Would be advantageous if accomplished; reduces system BOP

- Requires additional cathode optimization work

Adjusting GDL PTFE content; ink PTFE content; GDL thickness, cathode flow field design

Table 8: Single Cell: Remaining Challenges

	W*h/L	MeOH Util.	mW/cm^2
IFDL (dry air)	133.1	47.8%	8.1
IFDL (64% RH)	580	48.5%	34.8

Nafion 117 MEA
4mg/cm2 Pt, PtRu black, CCM method
17.1M MeOH @ 0.025mLpm,
2.0A (80mA/cm2), 70°C,
200 sccm air

Long term lifetime evaluation

- Most experiments to date have been 100 hours or less in duration

- No significant degradation observed so far, longer tests needed

Stack Development

First experimental stack fabricated at GTI

- Performance was low due to confusion about operating conditions

- Anode flow delivery was not consistent with single cells

Bogdan now overseeing this effort directly

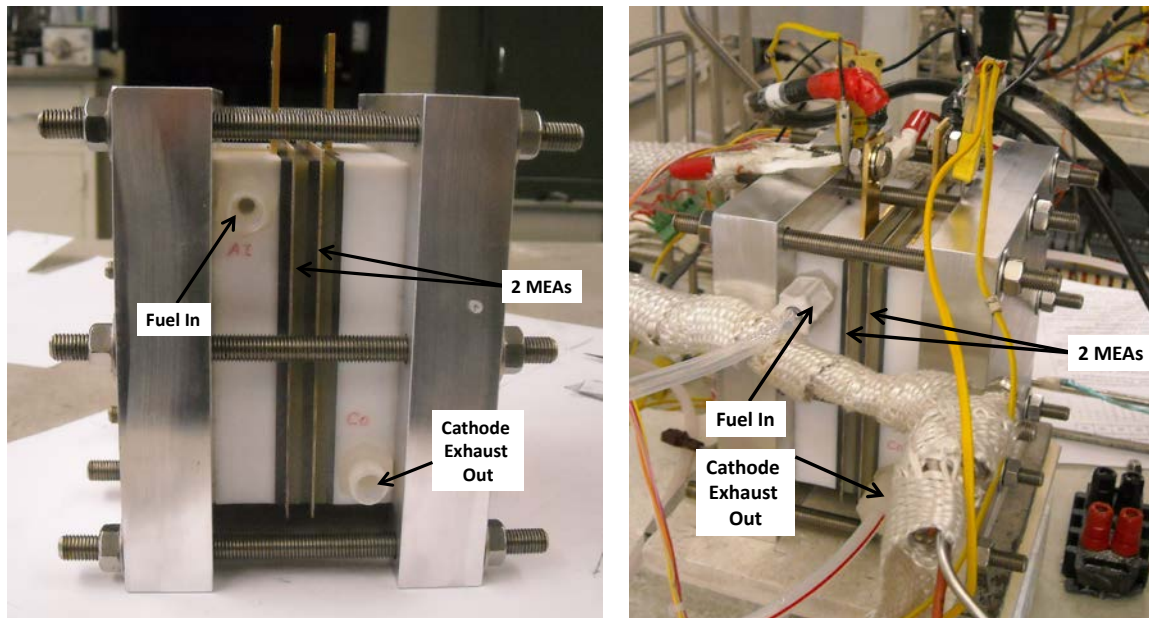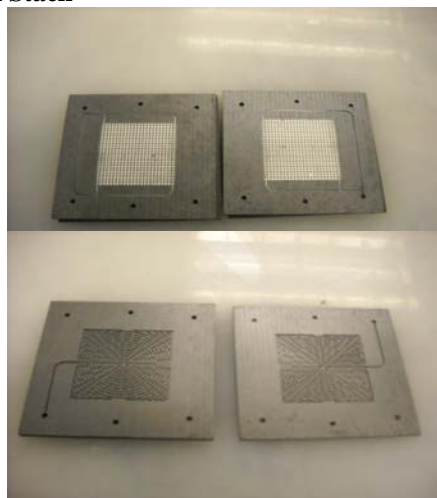- Improved results expected soon; materials supplied by NuVant as needed

Figure 14: First Experimental Stack

Experimental-Modeling Loop for air-side flow-field optimization

Reactant flow optimization is required for maximum performance of electrochemical flow reactors. A reactant stream will favor the path of least resistance, potentially starving regions of the electrode assembly and lowering reactor efficiency. Array fuel cells are ideal for evaluation of catalytic layers, gas diffusion layers, solid electrolytes, electrode fabrication methods and flow uniformity. The coupling of Array fuel cell analysis with a modular flow-field device that enables rapid variation of flow field configurations, and computational modeling, yields a powerful algorithm for flow optimization. Proper selection of the Reynold's number enables use of water for simulation of gas or liquid flow. Introduction of dye to the flow stream, with video recording, provides experimental data for a Navier-Stokes-based analysis of any flow-field configuration. Figure 1 shows our motivation for development of the flow optimization algorithm.
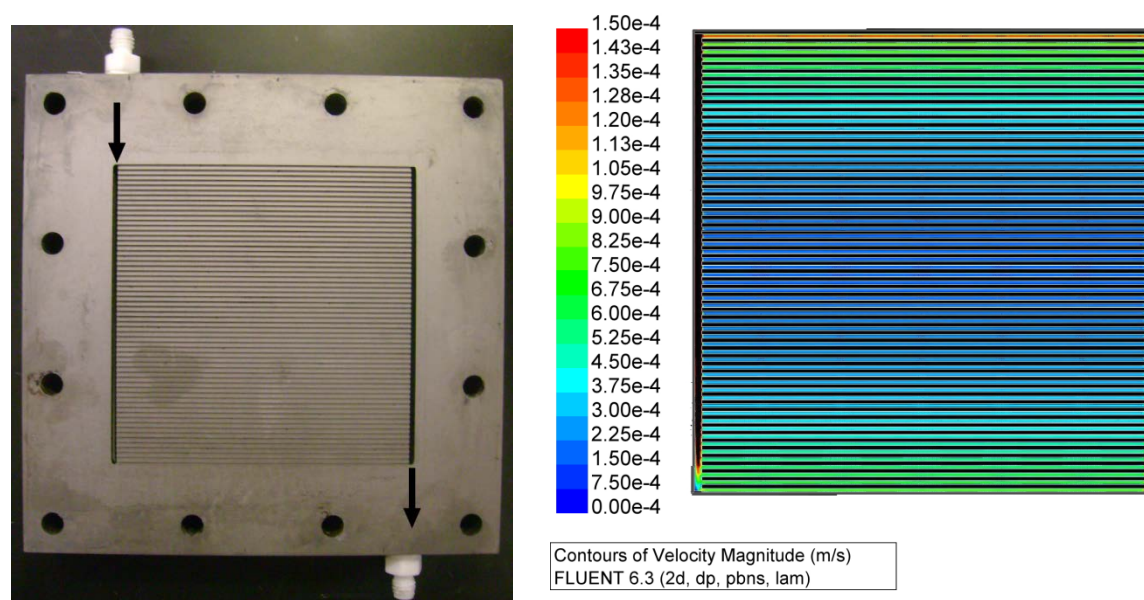

Figure 1. Left: Fuel cell flow field with inlet and outlet ports (arrows); Right: Steady state velocity contour map. Black regions (within vertical flow slots) indicate fluid velocity greater and out of range the color scale (adjusted for high resolution within the horizontal flow field region).

Inlet and outlet pin-fields are used to generate a uniform velocity front at a parallel flow field start-line. Figure 2 show a flow field provided by the subcontractor (GTI). A pin flow

field may be an option for programmatic IFDL cathodes. The Veriflow (Fig. 3) was developed to simplify variation of inlet and outlet pin-field configurations. Fluent™ (ANSYS, Inc. 275 Technology Drive, Canonsburg, PA 15317) computational fluid dynamics (CFD) software is used to down-select pin field configurations for Veriflow testing. CFD is also used to corroborate Veriflow™ results.


Figure 2: A parallel flow-field with inlet and outlet pin fields provided by GTI.

The modular Veriflow™ is dimensioned to simulate flow over a 100 cm² flow field. It allows installation of any flow-field, inlet, or outlet configuration compatible with a 100 cm² flow-field. It features interchangeable inlet and outlet housings, of various geometries, that accommodate interchangeable pin-boards (Fig 4.) for mass exchange of cylindrical (or any desired geometry) pins for build-up of candidate pin-field configurations.
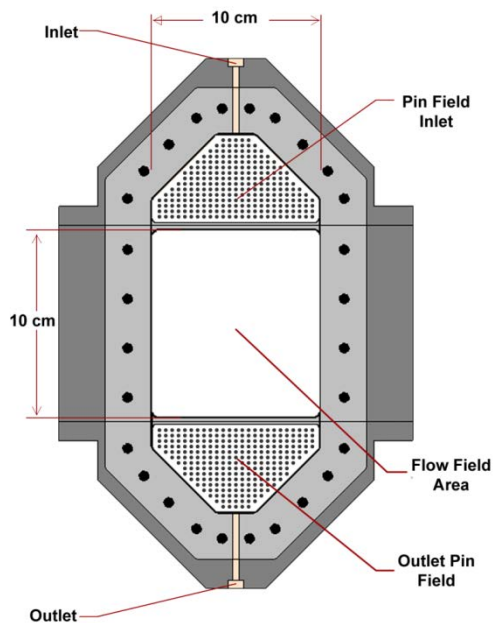

Figure 3: Veriflow™ schematic showing removable inlet and outlet pin fields and flow-field area.
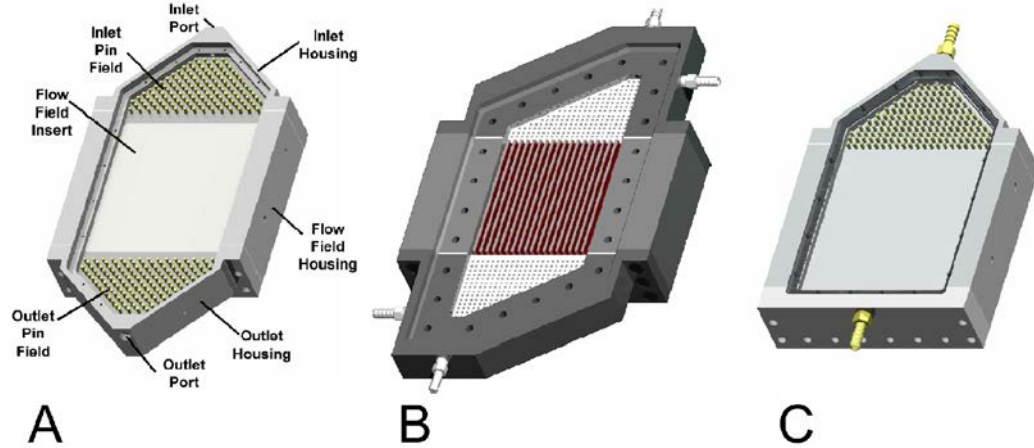
Figure 4: A. Basic Veriflow™ assembly; B. right triangle inlet/outlet housings with parallel flow field; C. Symmetrical triangular inlet with pin-less outlet.

The pin-board structure (Fig. 5 A) shows mating upper and lower pin-boards. The 1-pins, which insert through the top pin-board and bottom-out in the lower pin-board, serve to smooth out the top pin-board surface where flow obstruction is not desired. The insertion of the 2- and 3-pins is "stopped" by the larger diameter flow obstruction pin length. Any diameter pin or shape can be installed into the pin-board, provided that it has a 3/32" diameter mounting post. A set of .094", .125" and .150" outer-diameter pins were used for this work (Fig. 8B).
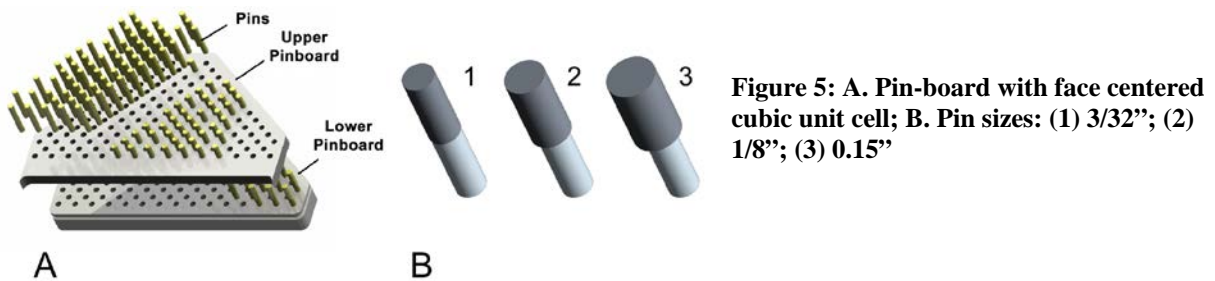
Figure 5: A. Pin-board with face centered cubic unit cell; B. Pin sizes: (1) 3/32"; (2) 1/8"; (3) 0.15"

Prior to dye injection the inlet and outlet ports, isolated by ball valves, are filled with water. The ball valves are opened and the syringe pump (charged with dyed water) delivers at a flow rate for direct, real-time viewing of flow characteristics. Figure 6 exemplifies time dependent flow of an un-optimized pin field at 60, 90 and 120 seconds from dye injection.
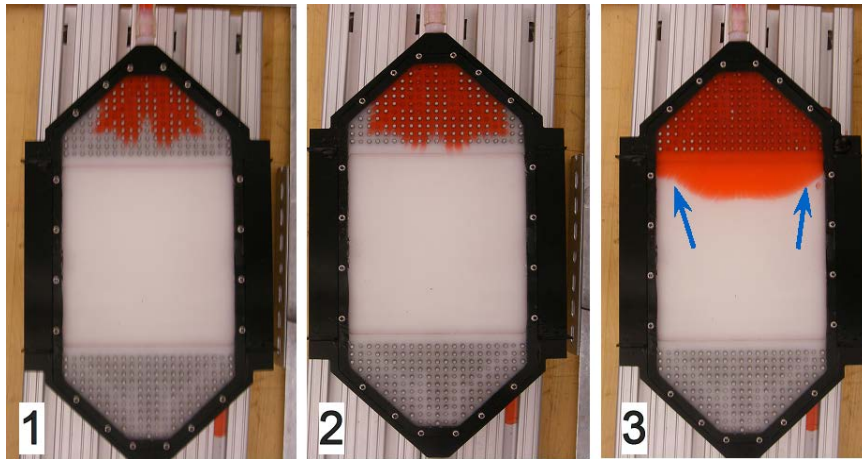
Figure 6. Arrows indicate areas of low flow. Images at (1) 60, (2) 90 and (3) 120 s from dye injection.
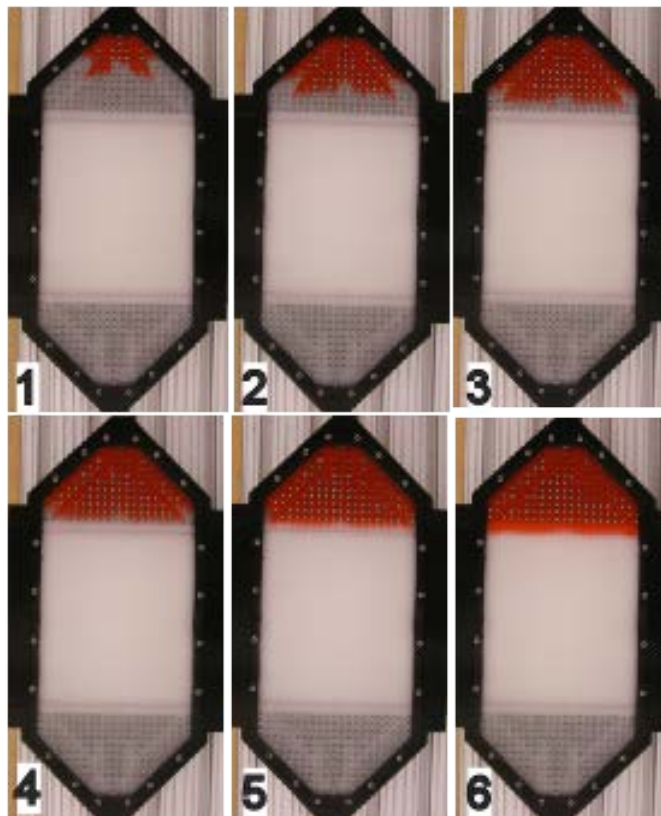

Figure 7. Pin-field after 4 additional Veriflow™ iterations. Images taken at 30, 60, 90, 100, 110, and 120 s (1 – 6) from dye introduction.

The modeling results used in the Veriflow feed-back loop are in a related DOE program focused on IFDL modeling. The concerted effort resulted in several iterations of the new

cathode flow field structure and array fuel cell builds. The latest iterations of the array fuel cells system are shown in Fig. 8a, 8b and 8c.
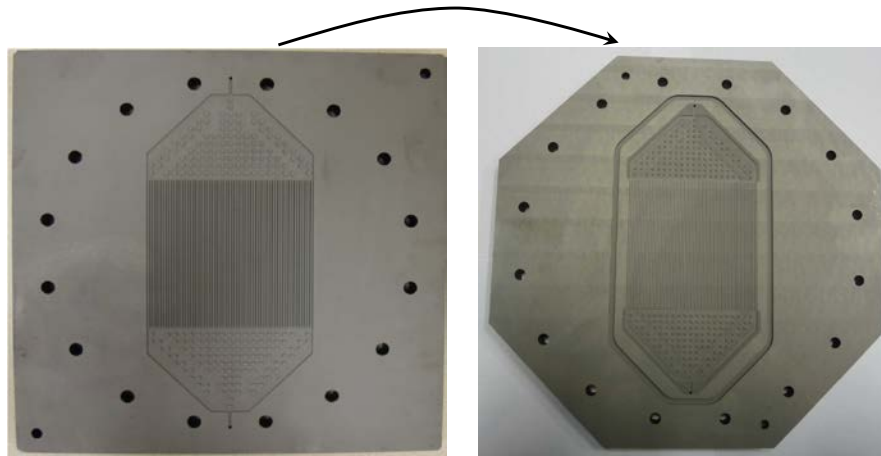
Figure 8a: Flow field pin field, developed from Veriflow-modeling effort, for uniform flow at a parallel flow field start line. The flow field is prepared in a configuration for Array fuel cell evaluation (left: old version, right: improved version).
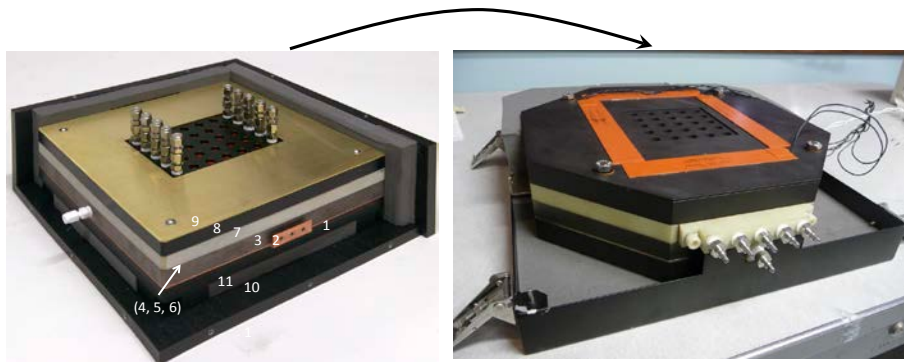
Figure 8b: Array fuel cell: placed in the heat insulated box (left: old version, right: improved version).
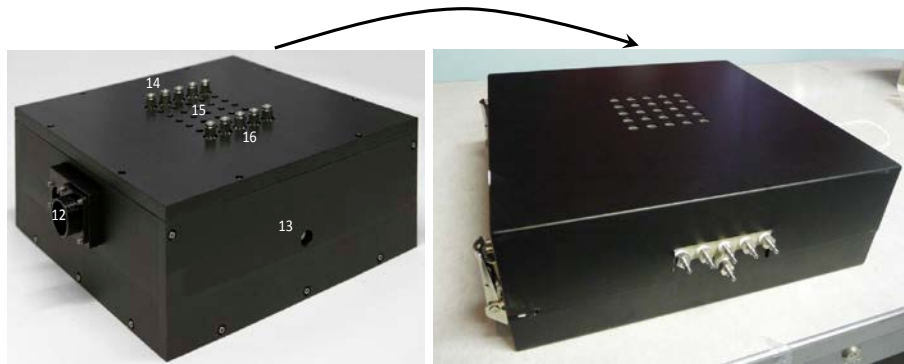
Figure 8c: Array fuel cell: assembled and sealed in the heat insulated box (left: old version, right: improved version).

The cathode flow field (Fig. 8a) was incorporated into a 25-channel Array fuel cell as the counter electrode to evaluate the test flow field in the absence of artifacts due to flow field sub-sectioning. An array membrane electrode assembly was prepared as reported by Liu et al.[1] A pressing jig was developed in order to obtain more precise force over each array electrode during the hot pressing of the gas diffusion electrodes to the Nafion membrane. The MEA is conditioned prior to data acquisition: Humidified N_2 was passed through the five parallel channels of the array-side flow field. The test flow field was switched to H_2, and O_2 was delivered to the array side. All gases (H_2, O_2, N_2) were at least 99.9 % with the exception of the 5 % CO balanced Ar. A high precision digital mass flow controller (Alicat Scientific, Inc., Tuscon, AZ) delivered to the test flow field (100 SCCM). The array column flow rates were regulated using a temperature controlled flow manifold with five pressure gauges and five high precision rotameters. The flow to each of the five flow field channels were set to 50 SCCM and calibrated using a soap-film flow meter (Bubble-o-meter, Dublin, OH).

Eleven Array system temperature regions were set as follows prior to start of experiments: test flow field (distant side from MEA) and humidifier transfer line 70 °C and 73 °C respectively, array flow field 60 °C, array-side transfer line 73 °C, array-side humidifier 70 °C and 5 array-side flow manifold transfer lines 73 °C.

To evaluate flow uniformity, humidified H_2 and O_2 were delivered to the test flow field and array side respectively. Data was acquired after overnight conditioning by scanning the 25 array electrodes simultaneously 80 times between 0.6 V and 0.95 V vs. the test flow field (i.e., dynamic hydrogen electrode).

After conditioning, steady state polarization curves were obtained from 0.35 V up to 0.95 V using a 'row switching technique': Data from one row is acquired while other rows are at open circuit, starting at row 5 and sequentially advancing to row 1. The 'row switching' method prevents upstream water production from affecting downstream electrodes and also eliminates O_2 reactant depletion effects. Data points were recorded after steady state attainment (ca. 60 s/point) to ensure uniform operating conditions at the array side. Cyclic voltammetry was acquired by swapping O_2 for N_2 on the array-side while H_2 was main-

tained at the test flow field. The electrodes were first cycled between 0.05 V and 1.2 V (vs. DHE), at 100 mV s^{-1} for 30 min.

Carbon monoxide (CO) stripping experiments were conducted after the CV pre-scans were reproducible. The array electrodes were dosed (5 % CO) at 0.05 V versus H$_2$ at the test flow field for 30 min to assure high and uniform coverage at the array-side: The flow field was then purged (N$_2$, 15 min) before CO stripping waves were acquired between 0.05 V and 1.2 V.

The array electrode disks were numbered (1-25) starting at the upper left (column 1, row 1) and ending at the lower right corner (column 5, row 5) as shown in figure 9.

Results and Discussion

Cyclic voltammetry

Prior to CO dosing, CVs were obtained for all 25 electrodes. The CVs were collected in 'Row switching mode'. Practically identical CVs were obtained for all the electrodes (Fig 9). In addition to confirming that the Nafion™ membrane was uniformly hydrated and the catalysts were stable under the temperature, humidification and pressure conditions, the scans show that flow to the test flow field is uniform and likely not a major contributor to dispersion of the data of fig. 9.
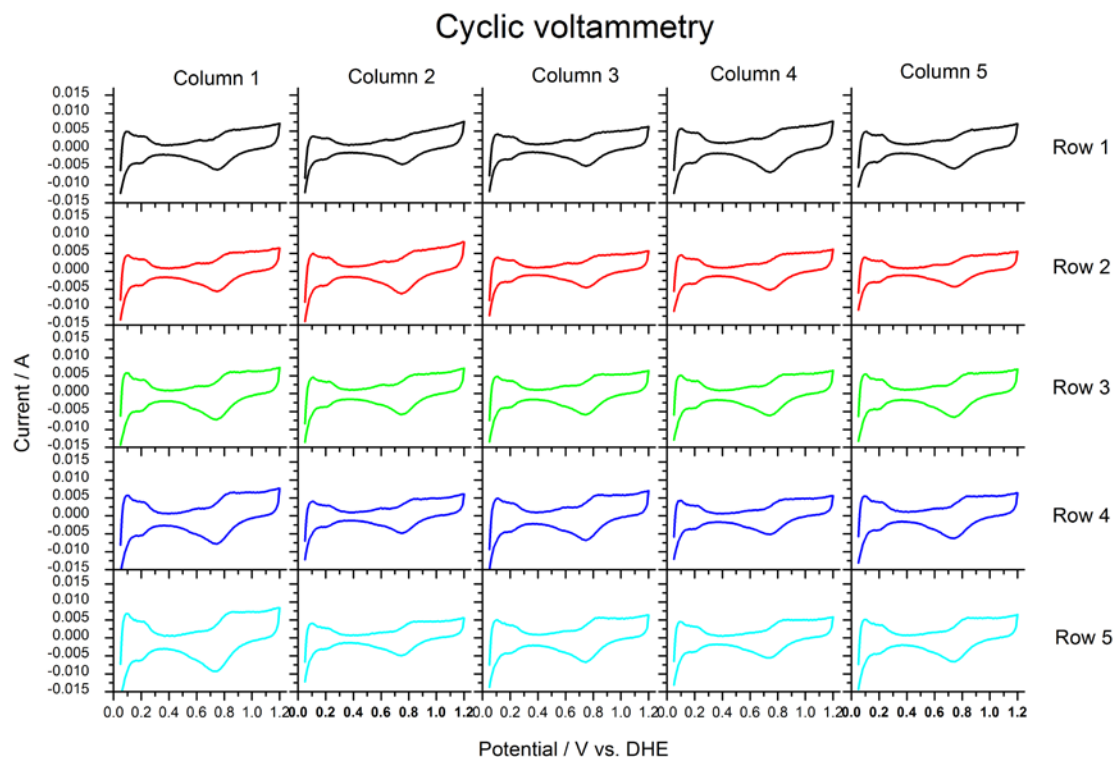
Figure 9 Cyclic voltammograms of 25 electrodes made of 40 wt. % Pt/C catalyst. The potential was cycled between 0.05 and 1.2 V vs. DHE. Experiments were carried out at 100 mV s^{-1} scan rate with 5 mV step size. The temperature of the system components: cell 60 °C, both humidifiers 70 °C. Hydrogen flow rate on the anode was set to 100 SCCM. Oxygen flow rates were around 50 SCCM for each parallel flow field.

CO stripping voltammetry

The follow-up CO stripping waves are presented in figure 10.
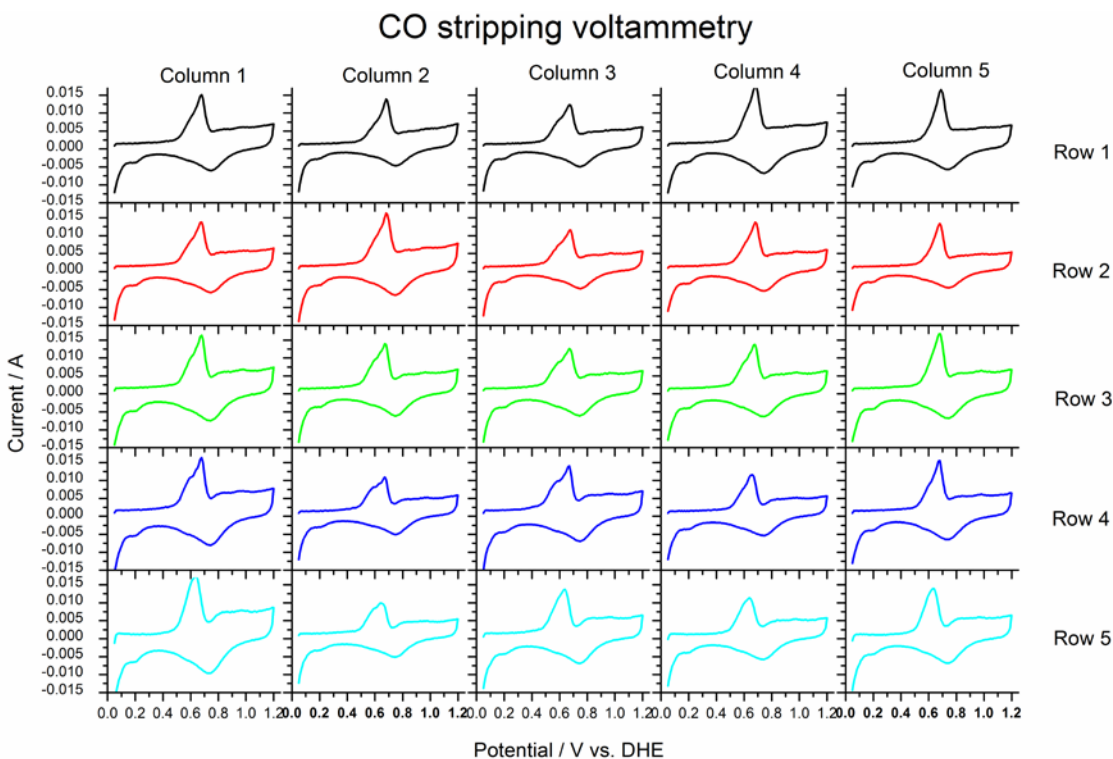
Figure 10. CO stripping experiment collected in 'Row switching mode'

The main stripping parameters are: CO stripping peak position, oxide reduction peak position and Pt 'real' surface areas. The peak potentials are presented in **Error! Reference source not found.**.

Table 9 CO stripping peak maximum position values for all 25 electrodes.

	CO stripping peak maximum position potential / V				
	Column 1	Column 2	Column 3	Column 4	Column 5
Row 1	0.680	0.675	0.680	0.680	0.680
Row 2	0.680	0.675	0.680	0.680	0.680
Row 3	0.680	0.670	0.670	0.675	0.680
Row 4	0.675	0.670	0.670	0.665	0.670
Row 5	0.660	0.660	0.660	0.660	0.660

The Pt oxide reduction peak position values from the CO stripping waves were near identical for all 25 CVs (i.e., ~ 0.75 V). Several of the stripping waves feature a shoulder on the low potential side of stripping wave. This may result from Ru crossover from test flow field electrode to the array side. This would shift CO stripping to more negative potentials.

Determination of electrochemically active Pt surface area

Figure 11 are representative array electrode data that shows the CO stripping wave (Scan 1, black solid line) and the well-defined H desorption region (Scan 2, red dashed line) used for Pt surface area calculations. A number of references discuss peak integration and Pt 'real' surface calculations.[2]
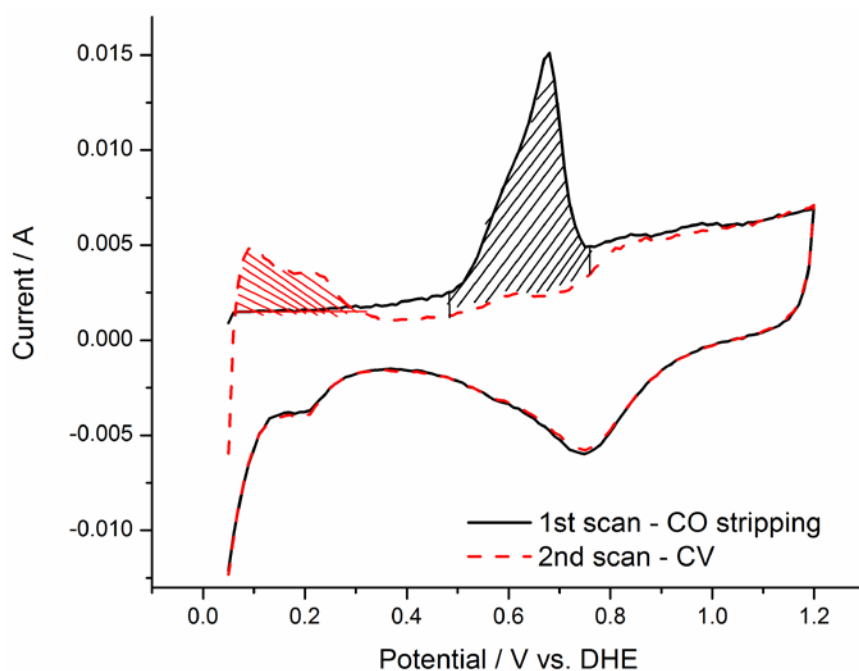

Figure 11 Peak area integration using: (a) hydride region desorption peaks (b) CO stripping peak.

The active area, using the CO stripping peak integral, was determined using **Error! Reference source not found.**.

$$\text{Pt}_{area}(cm^2_{Pt}) = \frac{\text{Measured CO stripping peak charge } (\mu C)}{420 \, (\mu C \, cm^{-2}_{Pt})} \qquad \textbf{Equation 1}$$

The hydrogen desorption (red striped area) is also used to calculate the surface area. The theoretical value of the charge associated with hydrogen and CO stripping is 210 μC cm^{-2} Pt and 420 μC cm^{-2} Pt respectively.

The active area calculated from the hydrogen desorption wave uses **Error! Reference source not found.**.

$$\text{Pt}_{area}(cm^2_{Pt}) = \frac{\text{Measured H stripping peak charge}\,(\mu C)}{210\,(\mu C\,cm^{-2}_{Pt})} \qquad \textbf{Equation 2}$$

The results obtained for the surface area calculations of both methods were similar. The average Pt 'real' surface area values for all 25 electrodes obtained from hydrogen desorption region was 28.30 cm^2 (S.D. ±5.02 cm^2) and from CO stripping peak was 27.81 cm^2 (S.D. ±4.05 cm^2). The standard deviation from CO stripping waves is lower than that obtained from the hydride desorption region.

Oxygen reduction polarization curves

The 25 polarization curves (Fig. 12), collected over a 5-hr time window to ensure steady state conditions, and were averaged to yield a benchmark curve. Column and row data were superimposed upon the benchmark (solid line) and are shown (Fig. 13).
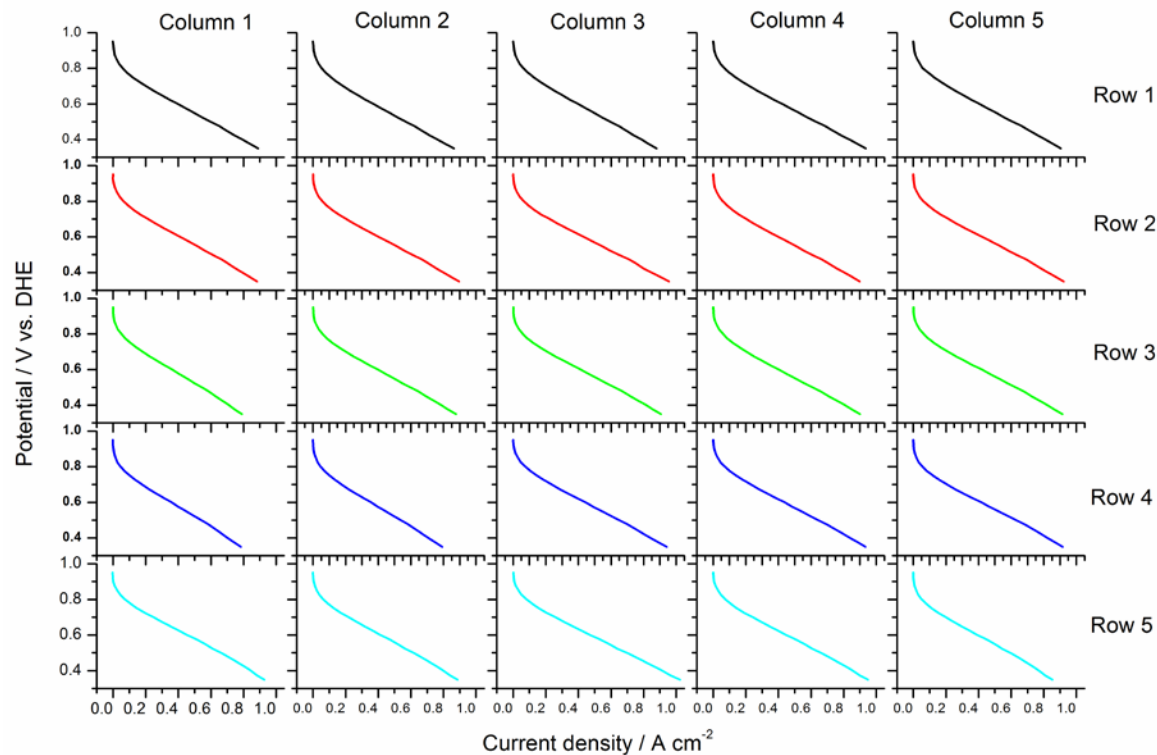
Figure 12. ORR polarization curves of array electrodes. 40 wt % Pt/C catalyst was used at the cathode/working electrodes. 40 wt % PtRu/C gas diffusion electrode (Johnson Matthey) was used at the test field electrode. System temperatures: cell; 60 °C, test field and array humidifiers; both 70 °C.
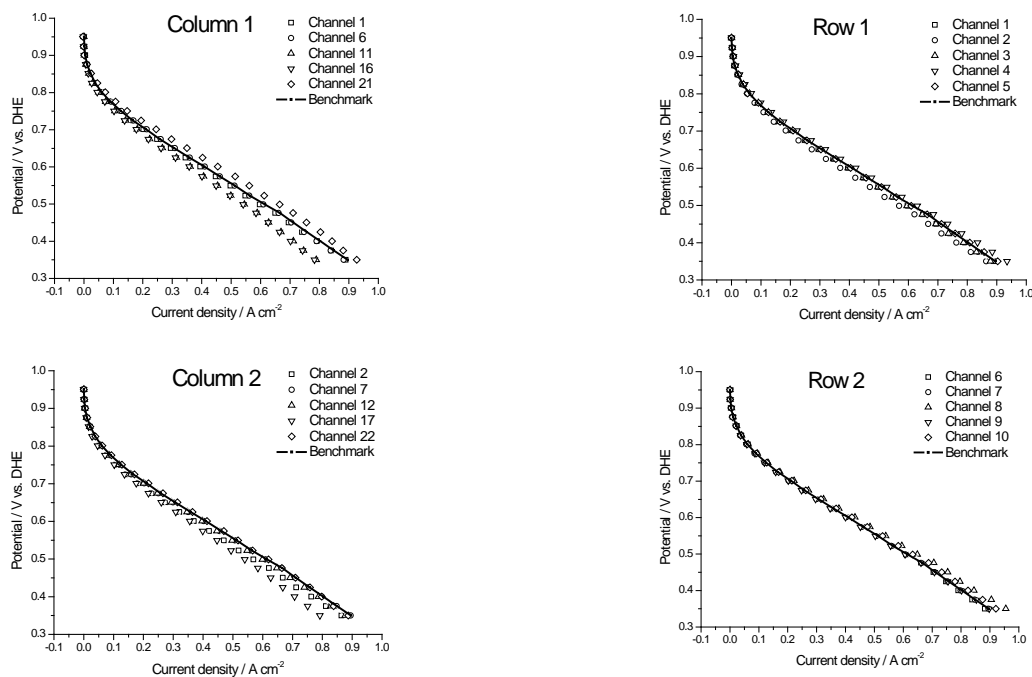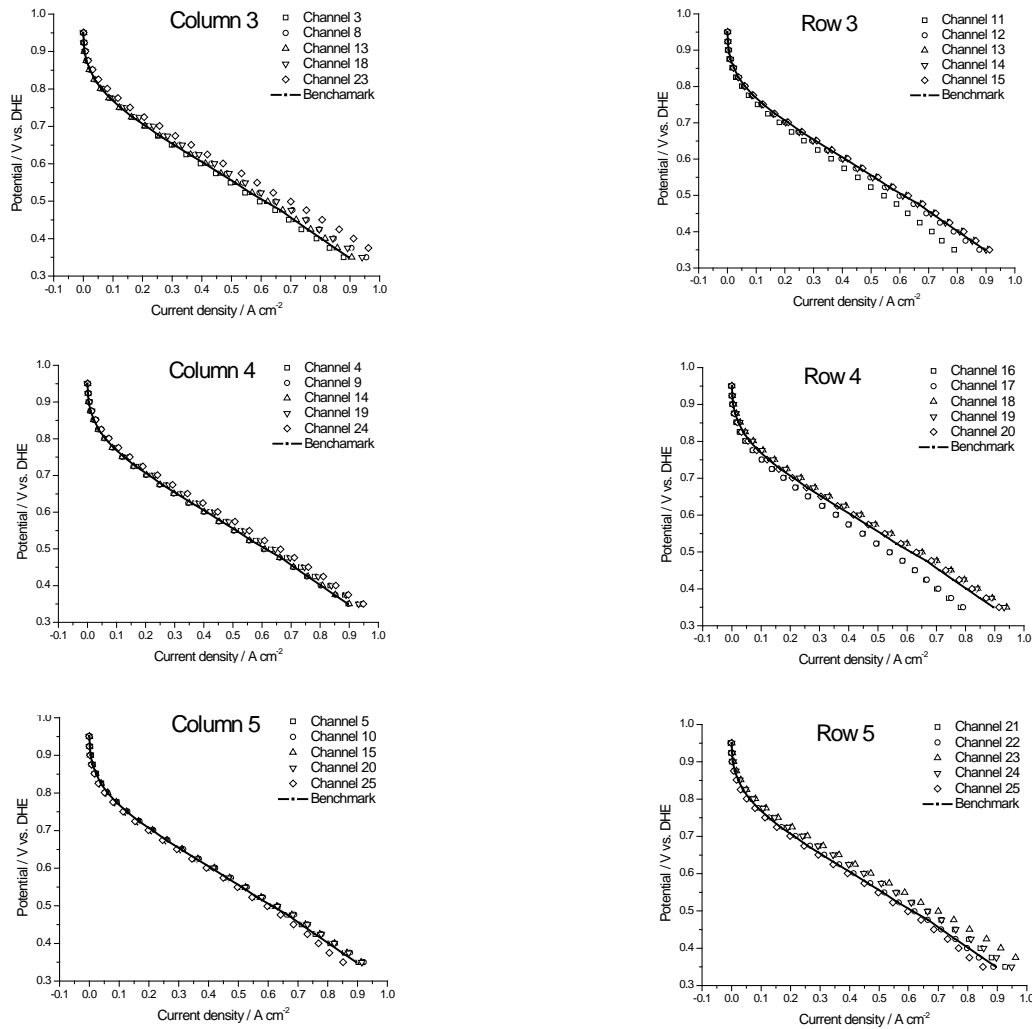
Figure 13 Column and row polarization curves superimposed upon the benchmark curve.

The column variations are somewhat higher than the row variations as expected. The array flow proceeds down the columns: column effects would be more likely than row effects from a design of experiments perspective. Figure 14 presents all the five columns' average polarization curves and all five rows' average curves results plotted against the benchmark.
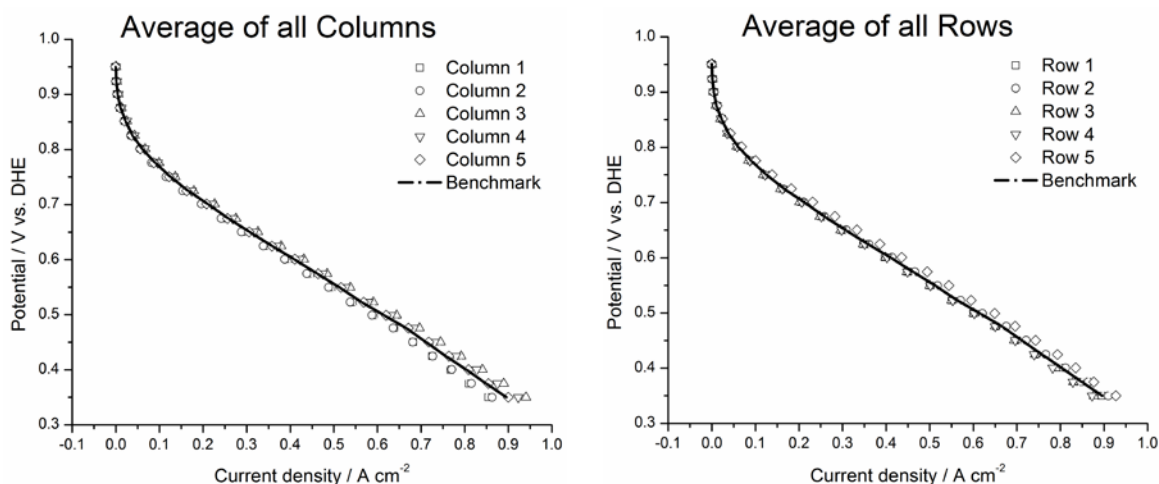
Figure 14. ORR polarization curves: (a) Column averages results and (b) rows average results superimposed upon the benchmark.

The array fuel cell results confirm the success of the Veriflow-modeling feedback loop for optimization of a pin field for a 100 cm² flow field. Incorporation of the flow field into the array fuel cell systems yielded the analysis results of this work.

Conclusions

The coupling of a modular pin field flow imaging device (Veriflow system) combined with Fluent™ modeling enabled rapid down-selection and confirmation of a parallel flow field. Array fuel cell CO stripping waves and fuel cell polarization curves, using the test flow field as a counter electrode, further confirmed that the iterative Veriflow process is a highly efficient algorithm of developing high-performance flow-fields. The end result of incorporation of the new pin field flow field into the Array fuel cell systems is a highly advanced high throughput screening system for flow electrochemical reactor components.

Laser Activated Membrane Introduction Mass Spectrometry (LAMIMS)

LAMIMS has the potential for discovery of bi-functional catalysts at the anode side of the fuel cell with characteristics: It may be required to partially reform fuel prior to electro-oxidation at the anode. The LAMIMS system is ideal for screening partial reforming catalysts for delivery of more efficient fuels to anode catalytic layers. The DOD contract funded Sara Evarts (NuVant co-op) at Northeastern University. LAMIMS hardware was funded by an ARO DURIP grant (S. Mukerjee). This component of the report exemplifies use of LAMIMS for evaluation of catalysts for methyl-cyclohexane dehydrogenation.

LAMIMS funding breakout:

1. $25,000 Mukerjee ARO DURIP funds for components
2. Additional equipment components were funded by NuVant (DOD contract)
3. One year of student co-op funded by NuVant Systems Inc. (DOD contract)

The LAMIMS has two main parts, the mass spectrometer and the reaction head connector. The system is designed for the attachment of a multitude of reaction heads, such as the LAMIMS reaction chamber or a Differential Electrochemical Mass Spectrometry (DEMS) reaction chamber, to the reaction head connector (Figure 1).
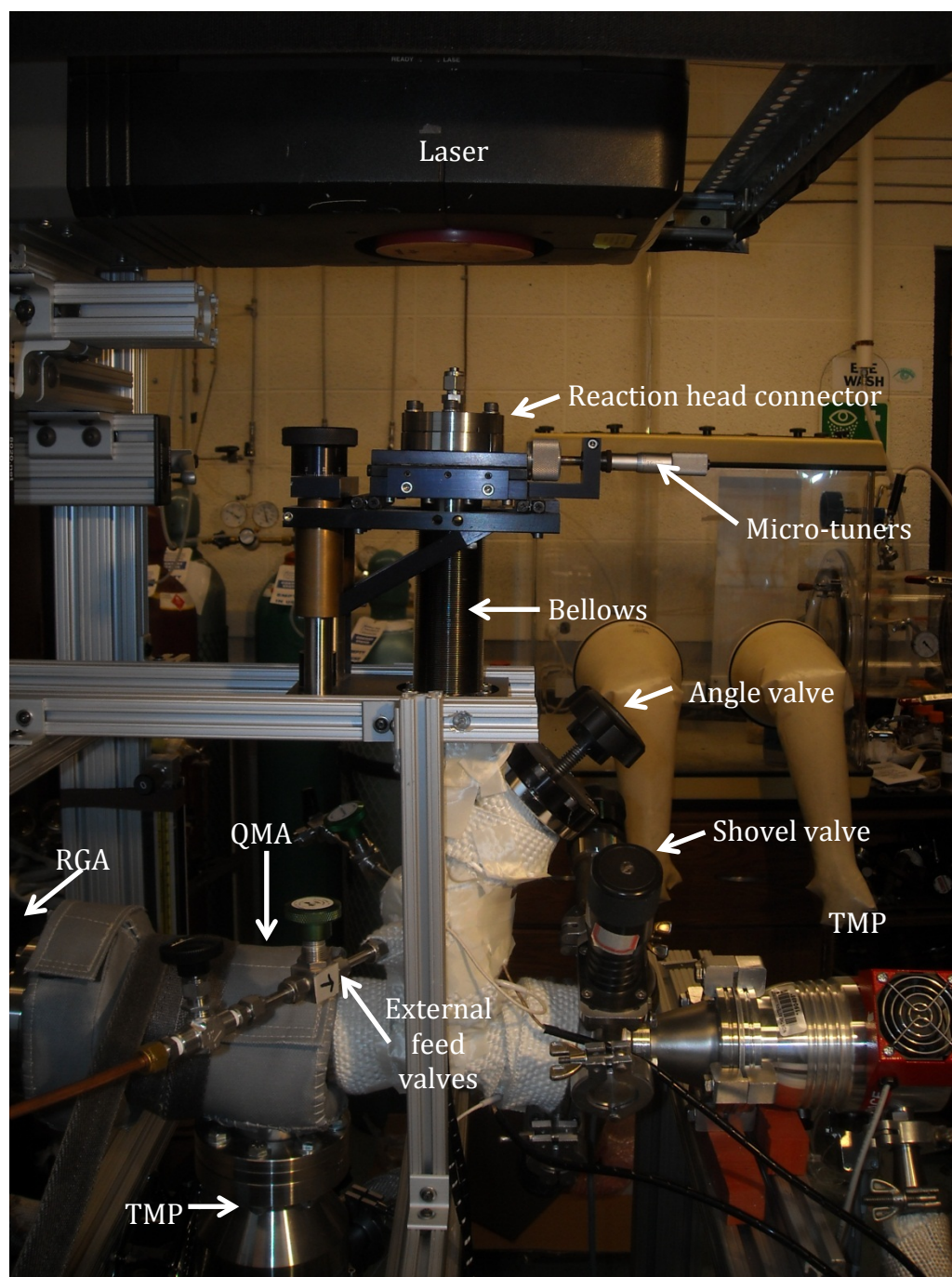
Figure 1. The LAMIMS system.

Figure 2 shows a top-view LAMIMS schematic. There are two roughing pumps (Edwards RV12 and Alcatel Pascal series pumps), each backing a turbomolecular pump (TMP). The two TMPs (Pfeiffer HiPace 80 and Alcatel PTM 5081) are on opposite sides of the vacuum system and are separated by the reaction head piece connector, which includes an angle valve, bellows, and stage flange. Two shovel valves are installed between the Pfeiffer TMP and the reaction head piece connector. These allow for isolation of the two TMPs and also provide ports for external device connection. A Pfeiffer PKR 251 Pirani cold cathode gauge is attached to one of the ports on one shovel valve. This allows for monitoring of the pressure in the high vacuum section of the system. The MKS Instruments 100D double open filament quadrupole mass analyzer (QMA) connects to an MKS Microvision 2 residual gas analyzer (RGA) and is between the reaction head piece connector and the Alcatel TMP, which actually sits below the QMA. A Humphrey 310 series solenoid valve is connected to the vacuum line between the Alcatel TMP and Alcatel roughing pump. The system is linearly connected as follows: Alcatel roughing pump, Humphrey solenoid valve, Alcatel TMP, QMA/RGA, reaction head piece connector, shovel valves, Pfeiffer TMP, Edwards roughing pump.

O-ring

Flange connector

Cap (Cu gasket)

Cap (O-ring)

Bottom connection

Microvision 2
RGA

QMA

PTM 5081
TMP

310
SV

V1

Pascal
Roughing
Pump

Head Piece Connector

Port 1

Port 2

V2 (Shovel)

V3 (Shovel)

Angle
Valve

Reducer

PKR 251
Gauge

Port 3

Port 4

Reducer

HiPace 80
TMP

Trap

TC2

RV12
Roughing
Pump

V4
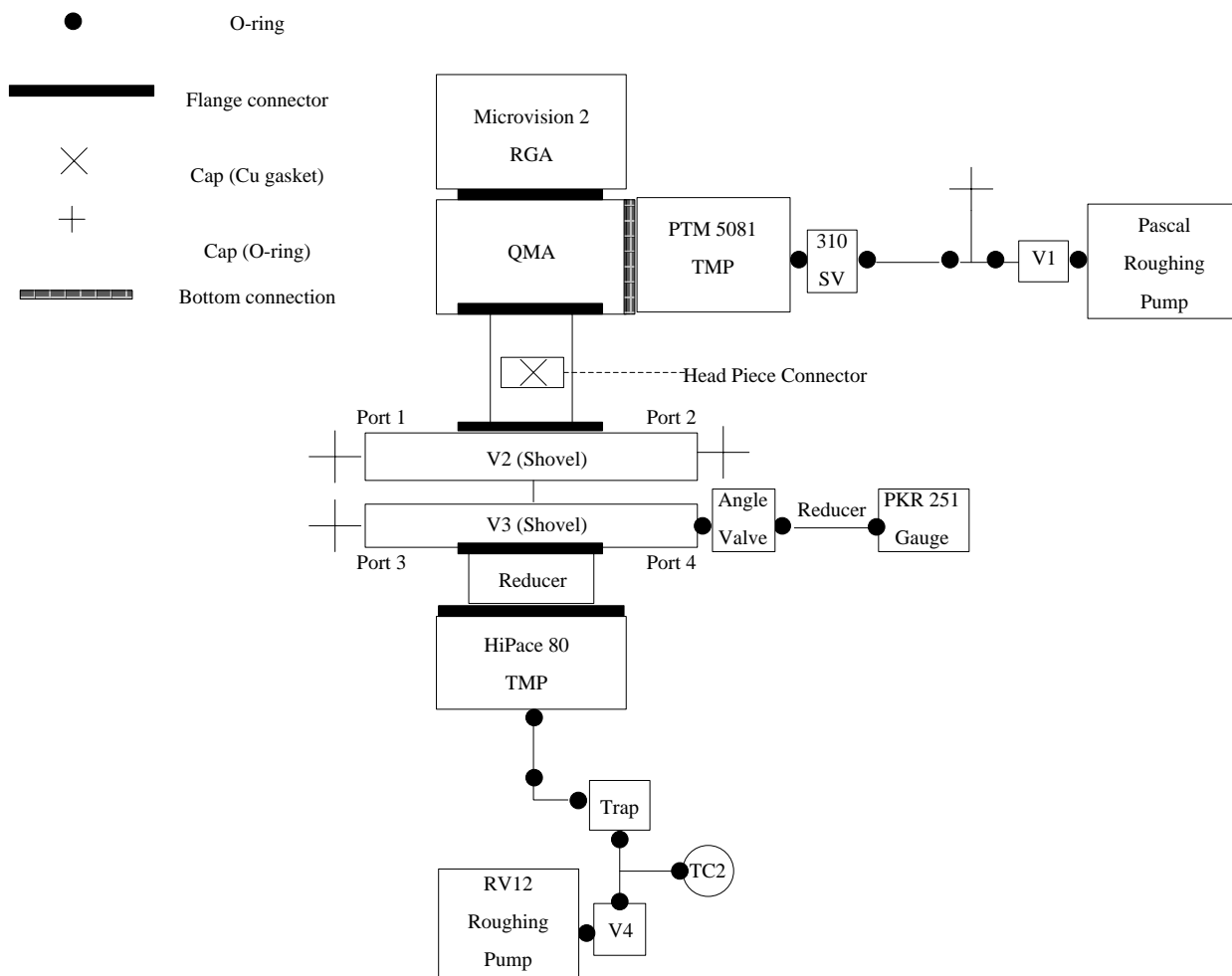
Figure 2 Schematic of LAMIMS

The reaction head connector extends vertically from the system. The bottom-most part is a flange with a small orifice in the center that limits the flow of products into the QMA. Above the orifice flange is another flange with an open center and two external feed valves. Above this is an angle valve, which isolates the reaction head from the external feed valves. This is followed by a bellows with two micro-tuners. The bellows allows for z-axis movement of the interchangeable reaction head stage, while the two micro-tuners provide the stage with x-axis and y-axis movement. Figure 1 shows a side view of the main parts of the LAMIMS system.

Most electronics are contained in a front panel on the LAMIMS system as seen in Figure 3: the Pfeiffer HiPace 80 DCU controller, the Alcatel CFV 100 TMP controller with connection to the solenoid valve, a computer, two thermocouple pressure gauge displays, and four temperature controllers. The entire system is contained on a custom built 8020 structure. There is an additional computer on the 8020 structure.

Figure 3 LAMIMS front panel. A professionally prepared front panel decal is under preparation.

42

Figure 4 shows sample data collected on the LAMIMS system. The reaction studied was dehydrogenation of methycyclohexane to toluene using Pt catalyzed beads. The data show the toluene partial pressures as a function of Pt loading on the ceramic beads. Catalytic beads were provided by UOP (Des Plaines, IL). An earlier version of the system has been previously reported[3]. This data will be published and attributed to the DURIP grant, UOP and the DOD contract[4].
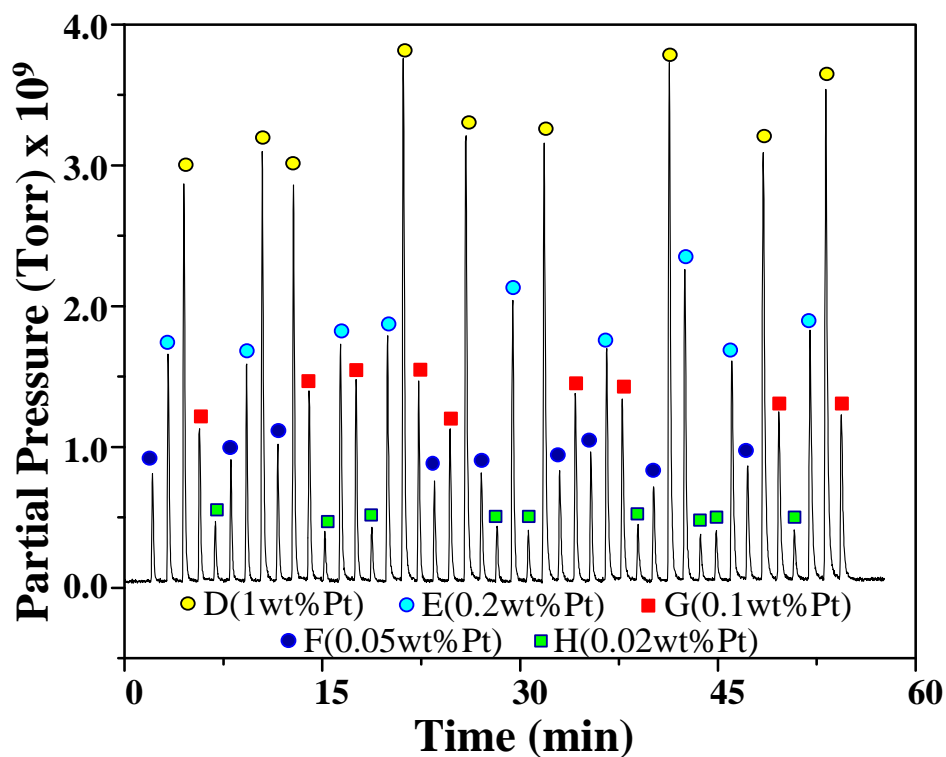

Figure 4 Peak height distribution of 45 bead catalysts randomly distributed on the carbon substrate.

DMFC MEA lifetime studies

Dunesh Kumari and Corey Grice carried out extensive lifetime analysis of MEAs operated in excess of 1000 hours. This work will be described in greater detail in a manuscript in preparation.

Future Work (internally funded)

- Single cell improvement/characterization

  – Thinner electrolyte (Nafion 211)

  – Cathode structure

  – Alkaline DMFC feasibility

- Stack development/optimization

  – Concurrent with single cell studies

1.   Liu, R.; Smotkin, E. S., Array membrane electrode assemblies for high throughput screening of direct methanol fuel cell anode catalysts. *Journal of Electroanalytical Chemistry* **2002,** *535* (1), 49-55.

2.   (a) Vidakovic, T.; Christov, M.; Sundmacher, K., The use of CO stripping for in situ fuel cell catalyst characterization. *Electrochim. Acta* **2007,** *52* (18), 5606-5613; (b) Lindstrom, R. W.; Kortsdottir, K.; Wesselmark, M.; Oyarce, A.; Lagergren, C.; Lindbergh, G., Active Area Determination of Porous Pt Electrodes Used in Polymer Electrolyte Fuel Cells: Temperature and Humidity Effects. *J. Electrochem. Soc.* **2010,** *157* (12), B1795-B1801; (c) McGrath, P.; Fojas, A. M.; Reimer, J. A.; Cairns, E. J., Electro-oxidation kinetics of adsorbed CO on platinum electrocatalysts. *Chem. Eng. Sci.* **2009,** *64* (22), 4765-4771.

3.   Nayar, A.; Liu, R.; Allen, R. J.; McCall, M. J.; Willis, R. R.; Smotkin, E. S., Laser-Activated Membrane Introduction Mass Spectrometry for High-Throughput Evaluation of Bulk Heterogeneous Catalysts. *Anal. Chem.* **2002,** *74* (9), 1933-1938.

4.   Rivera, H.; Evarts, S. E.; Nayar, A.; Kim, Y. T.; Rodriguez, J.; Galloway, D. B.; Falih, F.; Smotkin, E. S., Characterization and Modification of Laser Activated Membrane Introduction Mass Spectrometry (LAMIMS) System for Bead Catalysts. Manuscript in preparation.